

# A leptophobic massive vector boson at the Tevatron and the LHC

M. Heyssler<sup>1</sup>

*Department of Physics, University of Durham,  
Durham DH1 3LE, England*

## Abstract

Recent measurements of the single inclusive jet cross section at the Tevatron by the CDF Collaboration maybe suggest a modified picture of QCD in the large  $E_T$  range. One possible explanation of the measured jet excess is the introduction of a neutral heavy vector boson  $Z'$ . A parameter fit of this new model to the CDF data, in leading order perturbation theory, is performed, and the question of how the corresponding single inclusive jet cross sections and the dijet angular distributions at the LHC are affected by this additional  $Z'$  is discussed. We conclude that the  $Z'$  will play a pivotal role for typical LHC centre-of-mass energies, thus providing a direct test of this theory.

PACS numbers: 11.25.DB, 12.38.BX, 12.38.Qk, 12.60.Cn, 13.87.-a, 14.70.Pw

---

<sup>1</sup>email: M.M.Heyssler@durham.ac.uk

# 1 Introduction

Recent data from the CDF Collaboration [1] on the single inclusive jet cross section at the Tevatron indicate a possible disagreement with QCD at high transverse jet energies. The reported excess rate exceeds NLO QCD calculations by 10–50% for  $200 \text{ GeV} < E_T < 400 \text{ GeV}$ . One has to be cautious in drawing rash conclusions for the evidence of new physics, as the D0 Collaboration have reported *agreement* with QCD in the same measured jet energy range [2]. Still the systematic errors in both experiments are too large to enable definite conclusions to be drawn. But also the SLC and especially the LEP Collaborations [3] ALEPH, DELPHI, L3 and OPAL reported deviations measured in high precision experiments on the ratios  $R_{b,c} = \Gamma(Z \rightarrow b\bar{b}, c\bar{c})/\Gamma(Z \rightarrow \text{hadrons})$ . Compared to the predictions of the Standard Model, they find a too *large* value for  $R_b$  at about the  $3.5\sigma$  level and a too *small* value for  $R_c$  at about the  $2.5\sigma$  level. As  $R_b$  and  $R_c$  are correlated one might e.g. arbitrarily set  $R_c$  to the LEP1 experimental value, but the excess of  $R_b$ , now on a  $3.0\sigma$  level, remains.

Discussions continue on how to understand the CDF and (or) LEP1/SLC data from a phenomenological point of view if the disagreement with the Standard Model predictions is taken literally. For the CDF data there are efforts to explain the observed effects in terms of modified parton distributions [4], quark substructures, quark resonances or some more exotic models [5]. Independently the measured  $R_{b,c}$  values were treated in the framework of various extensions to the Standard Model [6]. However, in two recent publications by Altarelli *et al.* [7] and Chiapetta *et al.* [8] both CDF and LEP1/SLC data are treated on the same level and are described by a universal effect: the introduction of an additional very massive neutral vector boson coupled to the neutral quark sector of the Standard Model. This  $Z'$  boson has the feature that it couples very strongly to  $u$ - and  $d$ -type quarks and contributes to the standard boson  $Z$  decay via a weak  $Z'$ - $Z$  mixing angle  $\xi$ . Analysing the experimental data of the CDF and LEP1/SLC Collaborations allows a global parameter fit of the  $Z'$  model, and it was shown in Ref. [7] that a best-fit set of parameters can be found, to explain simultaneously the CDF jet data and the measured  $R_{b,c}$  values.

We shall exploit this idea and undertake a global analysis of the  $Z'$  model in the context of the CDF data only, to show the differences with the results of Refs. [7, 8] if one only takes the CDF data into account. But the main intention of this paper is to present predictions of the  $Z'$  model for further measurements at the Tevatron, like dijet angular distributions, and of course at the LHC  $pp$ -collider. As the  $Z'$  model seems a quantitatively plausible description of the observed deviations so far, it is important to give predictions for future experiments to either support or discard this explanation.

To give a brief outline of this paper, we discuss the  $Z'$  model in Section 2 and introduce its parametrisation. Section 3 focuses on the present and future data at the Tevatron. We fit the  $Z'$  model parameters to the CDF jet data and, as a first application, give predictions

for the dijet angular distributions in LO QCD with the  $Z'$  contribution included. In Section 4 we apply our *best-fit*  $Z'$  model to the LHC. Again we calculate the single inclusive jet cross sections and the dijet angular distributions. Finally, Section 5 summarises our results, underlines the most important features and discusses open problems.

## 2 The $Z'$ model

The  $Z'$  model introduced by Altarelli *et al.* in Ref. [7] and independently by Chiapetta *et al.* in Ref. [8] to explain recent experimental deviations from the Standard Model, has the remarkable feature (as the experimental data demand) that the axial and vector couplings of the  $Z'$ , especially to  $u$ -type quarks, are quite large. It will turn out that the effective  $Z'u\bar{u}$  coupling is of the order of the strong (QCD) coupling constant  $\alpha_S$ . Especially for large energies (transverse jet energies  $E_T$ ) the contributions due to the additional  $Z'$  are becoming dominant and for a fitted set of coupling parameters will for example cure the measured jet excess. We shall be very cursory in the presentation of the  $Z'$  model as it is treated in almost complete analogy to the  $Z$  boson of the Standard Model and has been already broadly discussed in [7, 8, 9].

To introduce the  $Z'$ , the neutral sector of the Standard Model with the underlying  $SU(3)_C \times SU(2)_L \times U(1)_Y$  gauge group is extended by an additional term in the neutral-current Lagrangian

$$\begin{aligned} \mathcal{L}'_{\text{NC}} &= \frac{g}{\cos(\Theta_W)} J'^0_\mu Z'^\mu \\ &= \frac{g}{2 \cos(\Theta_W)} \sum_f \bar{\Psi}_f \gamma_\mu (v'_f + a'_f \gamma^5) \Psi_f Z'^\mu. \end{aligned} \quad (1)$$

The neutral current  $J'^0_\mu$  includes the axial  $a'_f$  and vector  $v'_f$  coupling strengths of the  $Z'$ . In the Standard Model there are three free coupling parameters for the  $Z$  boson: the left-handed coupling to the  $(u, d)_L$  doublets and the two right-handed couplings  $u_R$  and  $d_R$ . To preserve these degrees of freedom, we follow the quark family-independent parametrisation for  $u$ - and  $d$ -type quarks in [7] for  $a'_f$  and  $v'_f$

$$\begin{aligned} v'_u &= x + y_u, & a'_u &= -x + y_u, \\ v'_d &= x + y_d, & a'_d &= -x + y_d. \end{aligned} \quad (2)$$

All couplings to leptons are set to zero (leptophobic  $Z'$ ):  $v'_l = v'_\nu = 0$  and  $a'_l = a'_\nu = 0$ . In [7] this constraint was due to the fact that only deviations from  $R_b$  and  $R_c$  have been reported by the LEP1/SLC measurements. Apart from  $x, y_u$  and  $y_d$  there are two more parameters included in the  $Z'$  model: the mixing angle  $\xi$  between  $Z$  and  $Z'$  as well as the mass  $M_{Z'}$  of the  $Z'$ . With these parameters we can also fully determine the total decay

width of the  $Z'$

$$\Gamma_{Z'} = \frac{G_F M_Z^2}{2\sqrt{2}\pi} N_c M_{Z'} (v_f'^2 + a_f'^2), \quad (3)$$

where  $N_c$  is the number of quark colours and  $G_F$  denotes the Fermi constant.

From fitting various electroweak observables to the LEP1/SLC data and taking the CDF results into account, the authors of Ref. [7] find as best set of parameters:  $x = -1.0$ ,  $y_u = 2.2$ ,  $y_d = 0.0$  and  $\xi = 3.8 \cdot 10^{-3}$  with the  $Z'$  mass fixed in this analysis to be  $M_{Z'} = 1$  TeV. This parameter space gives the best numerical compromise to simultaneously obtain acceptable coincidence with the values for  $R_{b,c}$  and the measured CDF jet rate. Such a heavy vector boson is in accordance with the lower mass limit of 412 GeV (at a 95% confidence level) reported from  $p\bar{p}$ -collider experiments in a search for a new neutral vector boson (with standard couplings) [10]. The dependence on the  $y_d$  parameter was found to be weak [7], such that the somewhat arbitrarily choice of  $y_d = 0.0$  was used as an input. We shall exploit these results and concentrate on finding the best set of parameters for  $x$  and  $y_u$  describing the CDF data within the  $Z'$  model, with  $\xi$ ,  $y_d$  and  $M_{Z'}$  fixed to the values given above<sup>2</sup>.

### 3 Fit to the CDF single inclusive jet data

In this section we shall perform a global  $\chi^2$  fit of the  $Z'$  model parameters  $x$  and  $y_u$  discussed in Section 2 to the 1992–93 measurements of the single inclusive jet cross section by the CDF Collaboration [1].

In leading order (LO) QCD the process  $AB \rightarrow jet + X$  can be parametrised by [11]

$$\begin{aligned} \frac{d^2\sigma}{dE_T d\eta}(AB \rightarrow jet + X) &= 4\pi\alpha_S^2(Q^2) \frac{E_T}{s^2} \\ &\times \sum_{abcd} \int_{x_a^{\min}}^1 \frac{dx_a}{2x_a - x_T e^\eta} \frac{f_{a/A}(x_a, Q^2)}{x_a} \frac{f_{b/B}(x_b, Q^2)}{x_b} |\overline{\mathcal{M}}_{ab \rightarrow cd}|^2, \end{aligned} \quad (4)$$

in terms of the transverse energy  $E_T$  of the observed jet and the directly measured pseudorapidity  $\eta$ . The expressions for the squared and averaged matrix elements of the subprocesses contributing to  $|\overline{\mathcal{M}}_{ab \rightarrow cd}|^2$  in LO due to the partons  $a, b, c$  and  $d$  being quarks, antiquarks or gluons, can be found in e.g. [12] or any standard QCD textbook. We integrate over the kinematical variable  $x_a$  only, with  $x_b = x_a x_T e^{-\eta} / (2x_a - x_T e^\eta)$  and  $x_a^{\min} = x_T e^\eta / (2 - x_T e^{-\eta})$ . The variable  $x_T$  is the scaled counterpart of  $E_T$  being  $x_T = 2E_T / \sqrt{s}$ . Eq. (4) fully describes the single inclusive jet cross section. For the

---

<sup>2</sup>As we restrict ourselves to fitting the CDF data only, the mixing angle  $\xi$  does not appear as a free parameter. However, because we later want to calculate  $R_{b,c}$  for the sake of comparison with the Standard Model predictions and the LEP1 data, we shall fix  $\xi$  to the value given by Altarelli *et al.* [7].

parton distributions  $f_{(a,b)/(A,B)}(x_{(a,b)}, Q^2)$  we use the MRS(A') set of partons described in Ref. [13].

The inclusion of the  $Z'$  into the formalism is straightforward. One has to calculate those matrix elements in which the incoming and outgoing partons are quark and antiquark pairs. The only constraints at the  $Z'q\bar{q}$  vertices are colour-charge and flavour neutrality. All possible  $Z'$  exchanges in the  $s$ - and  $t$ -channels have to be taken into account (cf. Fig. 1). The analytic expressions for these amplitudes are for example cited in [7, 9] and will not be repeated here.

Throughout this work we shall restrict ourselves to the LO calculation of the jet cross sections. For small values of  $|\eta|$  it has been shown in e.g. [14] that for single inclusive jet production at high transverse energies the next-to-leading order (NLO) and the LO calculations only differ by a constant factor, independent of  $E_T$ , if one chooses  $\mu = E_T/2$  as the underlying renormalisation scale. This renormalisation scale is imbedded into our calculations in the form of the four-momentum transfer  $Q^2 = \mu^2$  as the defining scale for the running coupling constant  $\alpha_S(Q^2)$  and the parton distributions. The difference between LO and NLO is then reported to be less than 10% and independent of  $E_T$  for  $E_T > 100$ –200 GeV [14]. The lower bound on  $E_T$  depends on the set of parton distributions used and the value of  $\Lambda_{\text{QCD}}$  implemented. For the MRS(A') set the QCD scale parameter is found to be  $\Lambda_{\overline{\text{MS}}}^{(N_f=4)} = 231$  MeV, which corresponds to  $\alpha_S(M_Z^2) = 0.113$  [13]. The MRS(A') NLO calculation was shown to be in good agreement [1] with the CDF single inclusive jet data up to  $E_T \simeq 200$  GeV. We therefore normalise our LO calculations of the single inclusive jet cross section to the CDF measurements in the range  $150 \text{ GeV} < E_T < 200 \text{ GeV}$  as shown in Fig. 2. The dashed curve represents the LO QCD calculation according to Eq. (4), the solid curve shows the *corrected* LO calculation normalised to the CDF data which are also presented. For  $130 \text{ GeV} < E_T < 200 \text{ GeV}$  the difference between the central values of the CDF data and the normalised LO calculation is less than 5%. The normalisation factor is found to be  $\mathcal{N} = 0.091 \pm 0.003$  according to the reported statistical errors of the CDF data. Comparing our results with those presented in [14] we conclude that for  $E_T > 130$  GeV and  $\mu = E_T/2$  our LO calculation is adequate to NLO assuming the constant factor  $\mathcal{N}$ . For our  $\chi^2$  analysis of the CDF data we shall therefore use the normalised LO calculation presented in Fig. 2.

The CDF Collaboration reported a significant jet excess for  $E_T > 200$  GeV [1]. In the inset of Fig. 2 we present the conspicuous deviations of the CDF data in the measured energy range to our LO calculation in per cent. The solid line shows the anticipated *best-fit* calculation in LO with the  $Z'$  incorporated and the smallest achievable  $\chi^2$  value. Let us therefore now briefly discuss our fit of the  $Z'$  model parameters  $x$  and  $y_u$  to the CDF data.

### 3.1 $\chi^2$ analysis of the $Z'$ model

The *qualitative* difference of our  $Z'$  model fit to that of Altarelli *et al.* [7] is that we only concentrate on the CDF data and disregard the values for the quark ratios  $R_b$  and  $R_c$  measured at the LEP1/SLC colliders for the moment. Furthermore we are using a different renormalisation scale ( $\mu = E_T/2$  rather than  $\mu = E_T$ ) and therefore approach NLO results in a natural way [14]. We also perform an implicit integration over the pseudorapidity  $\eta$  in the range  $0.1 \leq |\eta| \leq 0.7$ , more in line with the experimental cuts used by the CDF Collaboration.

Nevertheless we expect our *best-fit* parameters to be very close to those found in [7] such that we constrain three of the five parameters (cf. Section 2) in exact analogy to this work, namely  $\xi = 3.8 \cdot 10^{-3}$  (mixing angle),  $M_{Z'} = 1$  TeV ( $Z'$  mass) and  $y_d = 0.0$ . We are left with two parameters  $x$  and  $y_u$  to define the  $\chi^2$  distribution of our problem. We show  $\chi^2(x, y_u)$  in Fig. 3a. Note that the pure QCD calculation yields  $\chi^2(0, 0) = 45.14$ . Fig. 3b shows the 95.4% confidence ellipse ( $2\sigma$  for the normal distribution). The statistical analysis was performed using the programming package of Ref. [15]. While  $x$  is bound according to this analysis to a very narrow band, the parameter  $y_u$  covers a much broader range. The narrowness of the  $x$  range is due to the fact that it influences both  $u$ - and  $d$ -type quarks simultaneously, and therefore its variation is much more constrained.

Finally in Fig. 3c we present the 68.3% confidence ellipse ( $1\sigma$  for the normal distribution) and deduce the best-fit parameters of our analysis to be

$$\begin{aligned} x &= -1.0, & y_u &= 2.8, \\ \text{with } y_d &= 0.0, & M_{Z'} &= 1 \text{ TeV}, & \xi &= 3.8 \cdot 10^{-3}. \end{aligned} \quad (5)$$

Altarelli *et al.* [7] report a slightly smaller value of  $y_u = 2.2$ . This is mainly due to the included  $R_{b,c}$  fit as well as to the differences in the analysis procedure as discussed above. The improved result for the single inclusive jet cross section, due to incorporated  $Z'$  exchange with the parameters of (5), was already shown in the inset of Fig. 2. Note that with this set of parameters the coincidence with the experimental LEP1 values of  $R_b$  and  $R_c$  [3] is still better than the predictions by the Standard Model, as shown in Table 1.

With (5) and  $M_Z = 91.18$  GeV we find a total  $Z'$  decay width according to Eq. (3) of  $\Gamma_{Z'} = 644.2$  GeV. This should be compared to the value for the standard  $Z$  boson of  $\Gamma_Z = 2.493 \pm 0.004$  GeV [10]. Our value for  $\Gamma_{Z'}$  exceeds the one assumed by Chiapetta *et al.* [8] by a factor of three. From Eq. (2) we find the vector and axial couplings of the  $Z'$  to  $u$ -type quarks being  $v'_u = 1.8$  and  $a'_u = 3.8$ . These values should again be compared with the Standard Model predictions [10] of  $v_u = 0.19$  and  $a_u = 0.50$  for the  $Z$  boson. As already mentioned in Section 2, the effective  $Z'u\bar{u}$  coupling is of order  $(v'_u{}^2 + a'_u{}^2)\alpha_W \sim \alpha_S$ . So the main contribution of the  $Z'$  follows from its coupling to  $u$ -type quarks with an absolute strength that is comparable to QCD itself. The effects of this coupling can be observed in the inset of Fig. 2 where for  $E_T \sim 400$  GeV, the  $Z'$  contribution already

	our fit	LEP1	Standard Model
$R_b$	0.2194	$0.2219 \pm 0.0017$	$0.2156 \pm 0.0005$
$R_c$	0.1642	$0.1543 \pm 0.0074$	$0.1724 \pm 0.0003$

Table 1: Comparison of the values  $R_{b,c}$  from our calculation including the  $Z'$  model and the *best-fit* parameters of (5) with the LEP1 measurements [3] and the predictions of the Standard Model.

equals the pure QCD contribution.

Before we shall answer the question of how this  $Z'$  model with the new parameter fit will affect jet physics at the LHC we shall first discuss the comparison of our results to the already available and future data of the dijet angular distributions at the Tevatron.

### 3.2 Comparison with the measurements of the dijet cross sections at the Tevatron

The leading order differential dijet cross section in a hadron–hadron collision can be expressed in terms of the centre–of–mass scattering angle  $\cos(\Theta^*)$  and the invariant mass of the two jets  $M_{jj}$  [11]

$$\frac{d\sigma}{d\cos(\Theta^*)dM_{jj}}(AB \rightarrow jet_1 + jet_2 + X) = 4\pi\alpha_S^2(Q^2)\frac{1}{8M_{jj}^2} \quad (6)$$

$$\times \sum_{abcd} \int_{x_a^{\min}}^1 dx_a f_{a/A}(x_a, Q^2) f_{b/B}(x_b, Q^2) |\overline{\mathcal{M}}_{ab \rightarrow cd}|^2,$$

with  $x_a^{\min} = M_{jj}^2/s$  and  $x_b = M_{jj}^2/x_a s$ . Again  $a, b, c$  and  $d$  denote the different types of partons and  $A$  and  $B$  the scattering hadrons. The cross section is again factorised into one part that includes the information on the parton densities inside the hadrons and the averaged matrix element squared part that carries the  $\cos(\Theta^*)$  information. So the jet angular distribution is sensitive to the form of the  $2 \rightarrow 2$  matrix elements. For small angles, the partonic contributions to the total differential cross section show a typical Rutherford behaviour ( $\sim \sin^{-4}(\Theta^*/2)$ ). To remove this singularity it is convenient to plot

the angular distribution in terms of another variable  $\chi$  defined as<sup>3</sup>

$$\chi = \frac{1 + |\cos(\Theta^*)|}{1 - |\cos(\Theta^*)|}. \quad (7)$$

It is clear that  $\chi \in [1, \infty]$ . In the small angle region ( $\chi$  large) one expects therefore  $d\sigma/d\chi \sim \text{const.}$  as  $d\chi/d\cos(\Theta^*) \sim \sin^{-4}(\Theta^*/2)$ .

The vindication of restricting ourselves to a LO calculation has already been discussed in the case of the single inclusive jet analysis. We concluded that for  $E_T > 130$  GeV LO is a very good approximation to NLO (cf. Fig 2) if one chooses  $\mu = E_T/2$  as underlying renormalisation scale, and takes a normalisation factor  $\mathcal{N}$  into account. The dijet mass, however, is connected to the transverse jet energy via the relation

$$M_{jj} = 2E_T \cosh(|\eta^*|), \quad (8)$$

where we introduce the centre-of-mass pseudorapidity  $\eta^* = (\eta_1 - \eta_2)/2$  (with  $\eta_1$  and  $\eta_2$  being the pseudorapidities in the lab-frame).

With  $\cos(\Theta^*) = \tanh(\eta^*)$  and Eq. (7) we find that  $\chi = e^{2|\eta^*|}$ . Therefore Eq. (8) yields  $M_{jj} = E_T(\sqrt{\chi} + 1/\sqrt{\chi})$ . So one could expect that for large  $M_{jj}$  ( $M_{jj} > 260$  GeV) and small values of  $\chi$  our argumentation concerning the validity of the LO approximation might still hold. However, if there is a large transverse boost  $\eta_{\text{boost}} = (\eta_1 + \eta_2)/2$  to the dijet system then  $\chi$  can become as large as  $|\eta^*| = |\eta_1 - \eta_{\text{boost}}|$  but LO can still be adequate to NLO if  $|\eta_1|$  is small. On the other hand  $|\eta_{\text{boost}}|$  could be small and  $|\eta_1|$  large: in this case the LO description fails. So one has to be cautious with the argumentation. However Ellis *et al.* [16] also determined the scale  $\mu$  for which the calculation approximately reproduces the less scale dependent NLO result in the case of dijet production. If we express their result in terms of the variable  $\chi$ , one finds

$$\mu \approx k(\chi) \frac{E_T}{2}, \quad (9)$$

with  $k(\chi) = (\chi + 1)/(\chi^{0.85} + \chi^{0.15})$ . For  $\chi = 1$  we find  $\mu \approx E_T/2$ , the value for the renormalisation scale we were using throughout. We conclude that also in the case of dijet production this scale yields a reliable approximation to NLO (at least in the small  $\chi$  range). For  $\chi = 5, 10, 20$  one finds  $k(\chi) = 1.15, 1.29, 1.39$  such that nearly the complete range for small values of  $\chi$  is in approximate accordance with NLO for  $\mu = E_T/2$ . However, to approach the NLO result in a pure LO calculation as good as possible, we shall use the *effective* renormalisation scale of Eq. (9) for the study of the dijet angular distributions throughout this section. With this choice of  $\mu$  we do not have to worry about the normalisation factor  $\mathcal{N}$  introduced for the case of the single inclusive cross section.

---

<sup>3</sup>To minimise confusion we shall always denote the angular variable by  $\chi$  whereas the statistical variable is denoted by  $\chi^2$ .



We show in Fig. 4 our calculations in lowest order QCD as well as in the extended model (QCD+ $Z'$ ) with the coupled  $Z'$ . The  $Z'$  model parameters are again fixed to the values given in (5). We compare our results first with the data from the CDF Collaboration of 1992 [17]. They measured the jet angular distribution with a jet data sample of  $4.2 \text{ pb}^{-1}$  in three different dijet mass regions (Fig. 4a–c). Only the statistical errors are shown. The systematic errors are reported to be 5–10% [17]. The kinematical cut on the centre-of-mass pseudorapidity was chosen to be  $|\eta^*| < 1.6$  for  $240 \text{ GeV} < M_{jj} < 475 \text{ GeV}$  and  $M_{jj} > 550 \text{ GeV}$ ; and  $|\eta^*| < 1.5$  for  $475 \text{ GeV} < M_{jj} < 550 \text{ GeV}$ . Again with  $\chi = e^{2|\eta^*|}$  we get upper bounds for  $\chi$ , such as  $\chi < 24.5$  for  $\eta^* < 1.6$  and  $\chi < 20.0$  for  $\eta^* < 1.5$ . All cross sections in Fig. 4 are normalised to unity in the corresponding  $\chi$  intervals, and integrated over the given  $M_{jj}$  range. As the cross section falls very steeply in a given  $\chi$  bin ( $\propto 1/M_{jj}^3$ ), we introduce a cut-off for the dijet mass in Fig. 4c of  $M_{jj} = 700 \text{ GeV}$ . An analysis of the cut-off dependence showed that any higher upper bound on  $M_{jj}$  changes the result by less than 2%.

From a first look at Fig. 4 we notice that all angular cross sections are rising for higher values of  $\chi$ . This is due to the fact that we incorporated our running coupling constant  $\alpha_S(Q^2)$  with  $Q^2 = k^2(\chi)E_T^2/4$ . The  $Q^2$  scale is a function of  $M_{jj}$  and  $\chi$ . This can be deduced by examining Eq. (8). It follows directly that  $Q^2 = M_{jj}^2\chi/4(\chi^{0.85} + \chi^{0.15})^2$  with  $Q_{\text{max}}^2 = M_{jj}^2/16$ . For larger values of  $\chi$  the values of  $Q^2$  are therefore becoming smaller. The partons are probed at lower energies, but the effective coupling  $\alpha_S(Q^2)$  is rising as  $Q^2$  is shrinking.

A second feature becomes transparent from Fig. 4: the influence of the  $Z'$  is less striking for small and moderate dijet masses as shown in Fig. 4 but becomes more important for higher values of  $M_{jj}$ . We have to recall that a dijet mass of  $M_{jj} = 500 \text{ GeV}$  for  $\chi = 2.5$  corresponds to a transverse jet energy  $E_T = 226 \text{ GeV}$ , whereas a dijet mass of  $M_{jj} = 1000 \text{ GeV}$  corresponds to  $E_T = 452 \text{ GeV}$  for the same value of  $\chi$ . The  $Z'$  model, however, has been constructed in such way that its influence is only felt for  $E_T > 200 \text{ GeV}$ . Therefore only calculations with a relatively high dijet mass at  $\sqrt{s} = 1.8 \text{ TeV}$  are substantially affected by the  $Z'$  boson. But already for  $\langle M_{jj} \rangle = 500 \text{ GeV}$  and  $\langle M_{jj} \rangle = 600 \text{ GeV}$  the presence of the additional  $Z'$  becomes transparent (cf. Fig. 4b,c), especially for the large-angle-scattering ( $\chi$  small). This is due to the fact that such a massive vector boson acts like an effective contact interaction [18] (Fig. 1) between the four quarks at small energy transfers in the  $s$ - and  $t$ -channels. As, for example,  $|t| = M_{jj}^2/(\chi + 1)$  we obtain  $|t| \ll M_{Z'}^2$ , if  $\chi \gg 1$  and  $\mathcal{O}(M_{jj}^2) \simeq \mathcal{O}(M_{Z'}^2)$ . Because of the general form of the  $Z'$  matrix elements squared,  $|\overline{\mathcal{M}}_{Z'}|^2 \propto 1/((t - M_{Z'}^2)^2 + M_{Z'}^2\Gamma_{Z'}^2)$  [7, 9], we find the  $Z'$  contribution becoming flat for large  $\chi$ . Therefore the observed enhancement of the dijet cross sections due to this additional vector boson only takes place for small values of  $\chi$ .

The comparison with the CDF data should be regarded only as being illustrative, as for larger values of  $\chi$  the NLO and LO calculations slightly differ. The main purpose of Fig. 4 is to show the influence of the  $Z'$  on the pure QCD calculations. As we expected from the

*a priori* construction of the  $Z'$ , its presence is emphatically felt for higher dijet masses (like in Fig. 4c) mainly for large scattering angles where, with the choice of  $\mu = k(\chi)E_T/2$ , the authors of Ref. [16] observe that LO and NLO are quite comparable. This underlines the assumption given by Altarelli *et al.* [7] that the ratio  $Z'/\text{QCD}$  should merely remain unchanged (up to a few percent) in a transition to NLO.

To emphasise the influence of the  $Z'$  even more, we increased in Fig. 5 the dijet masses up to the region of  $M_{Z'}$  itself. For  $M_{jj} = 1100$  GeV (Fig. 5b) we calculate for the dijet cross section in LO QCD:  $dN/(Nd\chi)|_{\text{QCD}} = 0.0363$  for  $\chi = 1.5$  ( $\Theta^* = 78^\circ$ ). The LO QCD+ $Z'$  calculation, however, yields a value of  $dN/(Nd\chi)|_{\text{QCD}+Z'} = 0.0610$ , which means an increase by a factor of 1.7 due to  $Z'$  exchange.

It will be very interesting to compare our predictions to future results from the Tevatron to decide whether the  $Z'$  model is a suitable description *if* an excess in the dijet angular distributions for higher dijet masses continues to be observed. But such an excess has to be expected after the single inclusive jet cross section measurements. Such a double check would of course underline the reliability of the experimental data as well as test the theoretical predictions by any other models. We would like to mention some still preliminary data taken by the CDF Collaboration [19]. The data are still limited to dijet masses for which the  $Z'$  contribution is not significantly standing out against the statistical and systematic errors, even though especially the statistical errors could be quantitatively further reduced. An analysis of these data<sup>4</sup>, which is not presented here, showed again the excellent agreement with a calculation in LO in combination with the renormalisation scale of Eq. (9).

The ratios  $Z'/\text{QCD}$  of our calculations are also presented in Fig. 5. This gives even stronger evidence for the fact that for higher dijet masses the  $Z'$  contribution especially governs the larger scattering angles whereas for small angles the ratios behave smoothly. This can be observed in Fig. 5b where  $|Z'/\text{QCD}|$  even shrinks for larger  $\chi$  such that one might conclude that for high dijet masses but very small scattering angles the  $Z'$  contribution becomes irrelevant. Even though the LO calculations are not quite compatible to NLO in the high  $\chi$  range [16], the corrections due to NLO are supposed to cancel, considering the ratios only, such that this observation should also hold in a NLO calculation.

We conclude this section with a comparison to recent very precise data from the D0 Collaboration [20]. In the measured dijet mass range  $175 \text{ GeV} < M_{jj} < 350 \text{ GeV}$  the effect of the  $Z'$  is of course negligible as we have learned from the CDF data. However, as this data are the most precise available at this stage, we might test our argumentation about the reliability of the LO calculations. It has been reported [20] that the data are significantly consistent with NLO QCD calculations. In Fig. 6 we present the D0 data and normalise our cross sections as before in the shown  $\chi$  range. We restrict ourselves to a

---

<sup>4</sup>I am indebted to C. Wei from the CDF Collaboration for providing me with these preliminary results.

presentation of the QCD+ $Z'$  results only, as the differences to pure QCD are not striking in this mass regime (cf. Fig. 4a). The numerical values of the calculation with  $\mu = k(\chi)E_T/2$  lie almost within the error bars. Recall that this choice of  $\mu$  is in good agreement with NLO according to [16]. A statistical analysis yields  $\chi^2 = 12.39$ , so the LO calculation satisfactorily describes the experimental data, exactly as has been claimed throughout this section. A picture of consistency emerges out of the comparison to the experimental data. The dashed line shows the result for the calculation with  $\mu = E_T/2$ . The similarity in  $\chi^2$  is an indicator of how reliably this scale is again working in approximating NLO results for large scattering angles.

For illustrative reasons we also present the result for a completely different renormalisation scale. This shows that a less dynamical scale like  $\mu = M_{jj}$  cannot describe the experimental results (the  $\chi^2$  value is also presented). The curve is nearly flat over the whole  $\chi$  range.

## 4 The $Z'$ at the LHC

The question we want to address in this section is how the  $Z'$  will influence the measured jet cross sections at the LHC. From our results of Section 3 we expect the influence to be generally enhanced due to a higher centre-of-mass energy of  $\sqrt{s} = 10\text{--}14$  TeV. This allows the observation of higher transverse energies  $E_T$  and dijet masses  $M_{jj}$ . On the other hand we expect the background contributions like Drell–Yan processes [21], production of mini-jets [22], diffraction[23], etc. to become larger such that the signal/background ratio for the  $Z'$  will be even more reduced. We constructed the  $Z'$  such that it does not couple to leptons, and Drell–Yan processes via  $Z'$  exchange have to be completely excluded. Another feature somehow obstructs the detectability of the  $Z'$  at the LHC: at a  $pp$ -collider and high centre-of-mass energies the main contributions to the two-parton jet events come from subprocesses involving gluons, like  $gg \rightarrow gg(q\bar{q})$  and  $gq \rightarrow gq$ . But the  $Z'$  does not couple to gluons. And as antiquarks only appear as sea quarks in the proton we expect the main contribution from the  $Z'$  at the LHC to come from the  $t$ -channel exchange (cf. Fig. 1).

In the following we shall perform *all* calculations in pure LO for  $\mu = E_T/2$  and expect the arguments of Section 3 to be still valid, namely a difference between LO and NLO for large jet energies by a constant factor only and an even better coincidence between LO and NLO in the case of dijet production. The latter has been checked numerically by employing again the renormalisation scale of Eq. (9) and the previous results stated in Ref. [16]. At least for the ratios (QCD +  $Z'$ )/QCD we do not expect evident differences to NLO, as NLO corrections are expected to cancel.

In Fig. 7a we present the results for the single inclusive cross section at the LHC for fixed  $\eta = 0$ . The inset shows the ratios  $Z'/\text{QCD}$  for two different centre-of-mass energies

as a function of  $E_T$ . We observe that for  $E_T \sim 1000$  GeV the contribution from the  $Z'$  matches the QCD one for both curves. The curves are then rising very steeply but the typical  $\propto E_T^4$  behaviour we observed in the inset of Fig. 2 for the Tevatron is suppressed for  $E_T \gtrsim 2500$  GeV. To understand the underlying mechanism for this observation we present in Figs. 7b,c the individual subprocesses  $ab \rightarrow cd$  for the QCD and the  $Z'$  calculation. For higher centre-of-mass energies the gluons play the pivotal role and dominate the matrix elements of Eq. (4).

At typical LHC energies the  $qg \rightarrow qg$  contribution dominates with about 40% of all other subprocess events. For still larger values of  $\sqrt{s}$  also the gluon-gluon fusion rate is linearly growing whereas the number of subprocesses including quarks or antiquarks as initial partons is diminished as shown in Fig. 7b. We also observe the ratio  $(q\bar{q})/(qg) = 4/9$  as predicted by perturbative QCD [24] in Fig. 7b.

The  $Z'$  does not couple to gluons and therefore the  $Z'$  contribution is rising more slowly for higher centre-of-mass energies as the gluons actually give the dominant contributions. The corresponding subprocesses governing the  $Z'$  contribution are shown in Fig. 7c. This explains two features observable in Fig. 7a: first, the ratio  $Z'/\text{QCD}$  is becoming flatter for higher values of  $\sqrt{s}$  and second, the main high transverse jet energy is carried by the gluons. The latter is a well known fact and was theoretically dealt with in Ref. [25]. The relative contributions of quarks and antiquarks to large  $E_T$  processes is small, which yields the observed smoothing in the ratios at larger  $E_T$ . Note the absolute scales in Figs. 7b,c. For  $\sqrt{s} = 10$  TeV the  $Z'_{(qq)}$  subprocess exceeds the corresponding QCD $_{(qq)}$  rate by a factor of five. Fig. 7c also demonstrates the predominance of the  $Z'$   $t$ -channel exchange compared to the  $s$ -channel exchange sketched in Fig. 1.

We also give predictions for the dijet angular distributions as we did for the Tevatron. Fig. 8a shows the results for a calculation with  $M_{jj} = 1000$  GeV and  $M_{jj} = 2000$  GeV again for the two different centre-of-mass energies. Unlike the presentations for the Tevatron we now show the *unnormalised* distributions for our best-fit parameters (5). Qualitatively we find the same results as for the Tevatron: the  $Z'$  boson most strongly influences the small  $\chi$  region (again we interpret the  $Z'$  acting as an *effective contact interaction* [18] in this regime (cf. Fig. 1), contracting its propagator to an effective four-fermion point-like interaction) and this effect is again enhanced for higher dijet masses. The corresponding ratios shown in Fig. 8b underline the conclusions already drawn for the Tevatron, but now on a much larger scale.

Because we have so far presented our numerical results for our best-fit values (5) only, we finally want to show the variations of the  $Z'$  impact due to upper and lower bounds in accord with our analysis. If we fix  $x = -1.0$ , as we found the central  $x$  value to be, then we get upper and lower bounds on  $y_u$  from our  $\chi^2$  analysis if we restrict our fit-acceptance to the 68.3% confidence ellipse shown in Fig. 3c. For  $x = -1.0$  we read off  $y_u \in [2.4, 3.2]$ . Fig. 9a shows the single inclusive jet ratios for the three different values of  $y_u = 2.4, 2.8$  and  $3.2$  being the lower bound, central value and upper bound respectively. The discrepancy

between the different choices of  $y_u$  becomes very striking for higher  $E_T$  values. The total decay width varies from  $\Gamma_{Z'} = 508.0$  GeV ( $y_u = 2.4$ ) up to  $\Gamma_{Z'} = 801.4$  GeV ( $y_u = 3.2$ ), which increases the phase space of the  $Z'$  especially at high transverse energies. So, large  $E_T$  measurements at the LHC might be an excellent probe to more precisely fix the value of  $y_u$ , as the cross sections are very strongly dependent on  $y_u$  in this energy range and so a clear  $y_u$  correspondence is achievable. The difference to the best-fit of Altarelli *et al.* [7] ( $y_u = 2.2$ ) is also shown. Note the difference of only 7% to our lower bound ( $y_u = 2.4$ ) for  $E_T = 3000$  GeV.

Fig. 9b finally shows the ratios  $Z'/\text{QCD}$  for the dijet angular distributions with the same values for  $y_u$  as in Fig. 9a. The  $Z'$  impact on the small  $\chi$  region is again significant. The extreme values of  $y_u$  differ by a factor of roughly two in the complete  $\chi$  range shown. Again, future measurements of the dijet angular distributions at the LHC might further determine  $y_u$  more exactly according to the large dependence of the ratios to the choice of this coupling parameter.

## 5 Conclusions

In this paper we exploited the idea suggested in Refs. [7, 8] to give predictions for a postulated new heavy vector boson  $Z'$  at the LHC. With this additional very massive boson it was possible to quantitatively explain the reported  $R_{b,c}$  anomalies from LEP1/SLC experiments as well as simultaneously the measured CDF jet excess rate. It was shown by above authors that the postulated vector boson must have three special features: it is leptophobic and couples very strongly, but family-independent, to  $u$ - and  $d$ -type quarks; it shows a weak mixing with the standard  $Z$  gauge boson in order to contribute to its decay widths  $\Gamma(Z \rightarrow b\bar{b}, c\bar{c})$  in particular; it is very massive with a typical mass of order  $M_{Z'} = 1$  TeV.

In this work we fitted the coupling parameters  $x$  and  $y_u$  of the  $Z'$  in a global leading order  $\chi^2$  analysis to the 1992–93 CDF data on the single inclusive jet cross sections. Although we find a slightly larger value for  $y_u$  than Altarelli *et al.* [7], we showed that our best-fit parameters are still in better accordance with the LEP1  $R_{b,c}$  measurements than the Standard Model predictions.

With this set of parameters we then gave predictions for the  $Z'$  effect on future precision measurements at the LHC. We showed the corresponding physical parameter ranges for which the influence of the  $Z'$  is expected to be most striking and besides *qualitative* considerations we also provided *quantitative* predictions for single inclusive jet cross sections and angular dijet distributions at the LHC. We presented numerical results for different coupling parameters  $y_u$  that were allowed on the 68.3% confidence level from our previous CDF data fit. This will help to further determine the free parameters of the  $Z'$  model as soon as first LHC data are available.

As a final critical remark we want to point out that despite the very precise and reliable experiments there might still be no compelling reason to look for *new physics*. However, future data are necessary, and the LHC will play a pivotal role as a high-energy laboratory and new theoretical models and predictions, rising from such fundamental contradictions to the Standard Model, will become important.

We did not try to answer the question of where the  $Z'$ , if it is indeed genuine, originates from. For an overview on several motivations for the existence of additional vector bosons and a list of the most studied models we refer to [26]. In addition we should mention a model for the neutral boson proposed in [27], where it originates from the breaking of an extended colour group, such as  $SU(4)_C$  or  $SU(5)_C$ . In this model the vector boson is very strongly coupled to  $q\bar{q}$  pairs and weakly coupled to leptons. As reported in [28] its mass should be larger than 600 GeV. In view of the proposed features this model could be a promising  $Z'$  candidate.

## Acknowledgements

First of all I would like to thank James Stirling for drawing my attention to this topic and for many fruitful discussions throughout. Chao Wei from the CDF Collaboration is thanked for making some preliminary data on the dijet angular distributions accessible to me, to cross-check the stated assumptions about LO approximations. I am indebted to John Campbell and Colin Weir for critical comments concerning the manuscript. Finally, financial support in the form of a “DAAD–Doktorandenstipendium” HSP–II/AUFE is gratefully acknowledged.

## References

- [1] CDF Collaboration: F. Abe *et al.*, ‘*Inclusive jet cross section in  $p\bar{p}$  collisions at  $\sqrt{s} = 1.8 \text{ TeV}$* ’, Fermilab preprint FERMILAB-PUB-96/020-E, 1996.
- [2] D0 Collaboration, talk presented by J. Blazey at the XXXI. Recontres de Moriond, March 1996.
- [3] The LEP Collaborations ALEPH, DELPHI, L3, OPAL and the LEP Electroweak Working Group, CERN preprint CERN-PPE/95-172, 1995.
- [4] CTEQ Collaboration: J. Huston *et al.*, ‘*Large transverse momentum jet production and the gluon distribution inside the proton*’, Michigan State U. preprint MSU-HEP-50812, FSU-HEP-951031, CTEQ-512, 1995.  
E.W.N. Glover, A.D. Martin, R.G. Roberts and W.J. Stirling, ‘*Can partons describe the CDF data ?*’, Durham U. preprint DTP/96/22, RAL-TR-96-019, 1996.
- [5] M. Bander, ‘*Quark resonances and high  $E_T$  jets*’, U. California (Irvine) preprint UCI-TR96-7, 1996.  
R.S. Chivukula, A.G. Cohen and E.H. Simmons, ‘*New strong interactions at the Tevatron ?*’, Boston U. preprint BUHEP-96-5, 1996.
- [6] E. Malkawi and C.-P. Yuan, Phys. Rev. **D50** (1994) 4462.  
D. Comelli, F.M. Renard and C. Verzegnassi, Phys. Rev. **D50** (1994) 3076.  
G.J. Gounaris, F.M. Renard and C. Verzegnassi, Phys. Rev. **D52** (1995) 451.  
F.M. Renard and C. Verzegnassi, Phys. Lett. **B345** (1995) 500.
- [7] G. Altarelli, N. Di Bartolomeo, F. Feruglio, R. Gatto and M.L. Mangano, ‘ *$R_b, R_c$  and jet distributions at the Tevatron in a model with an extra vector boson*’, CERN preprint CERN-TH/96-20, UGVA-DPT 1996/01-912, 1996.
- [8] P. Chiapetta, J. Layssac, F.M. Renard and C. Verzegnassi, ‘*Hadrophilic  $Z'$ : a bridge from LEP1, SLC and CDF to LEP2 anomalies*’, Marseille U. preprint PM96-5, CPT-96/P-3304, 1996.
- [9] P. Chiapetta and M. Greco, in Proceedings of the Large Hadron Collider Workshop Vol.II p.686, Aachen, 1990.  
H. Georgi, E. Jenkins and E.H. Simmons, Phys. Rev. Lett. **62** (1989) 2789.  
V. Barger and T.G. Rizzo, Phys. Rev. **D41** (1990) 946.
- [10] Particle Data Group, *Review of Particle Properties*, Phys. Rev. **D50** (1994) 1173.
- [11] G. Sterman *et al.*, Rev. Mod. Phys. **67** (1995) 157.

- [12] B.L. Combridge, J. Kripfganz and J. Ranft, Phys. Lett. **B70** (1977) 234.
- [13] A.D. Martin, W.J. Stirling and R.G. Roberts, Phys. Lett. **B354** (1995) 155.
- [14] S.D. Ellis, Z. Kunszt and D.E. Soper, Phys. Rev. Lett. **64** (1990) 2121.  
 W.T. Giele, E.W.N. Glover and D.A. Kosower, Nucl. Phys. **B403** (1993) 633.  
 W.T. Giele, E.W.N. Glover and D.A. Kosower, ‘*Next-to-leading order results in jet physics*’, in Proceedings of the 13<sup>th</sup> International Conference on Particles and Nuclei (PANIC ’93) p.201, Perugia, 1993.
- [15] B.P. Flannery, W.H. Press, S.A. Teukolsky and W.T. Vetterling, *Numerical Recipes in C* (Cambridge University Press), 1991.
- [16] S.D. Ellis, Z. Kunszt and D.E. Soper, Phys. Rev. Lett. **69** (1992) 1496.
- [17] CDF Collaboration: F. Abe *et al.*, Phys. Rev. Lett. **69** (1992) 2896.
- [18] E.J. Eichten, K.D. Lane and M.E. Peskin, Phys. Rev. Lett. **50** (1989) 811.
- [19] Preliminary results of the CDF Collaboration (C. Wei, private communication) from an analysis of 1992–93 (Run 1A) and 1993–95 (Run 1B) measurements.
- [20] H. Weerts, in Proceedings of the 9<sup>th</sup> Topical Workshop on Proton–Antiproton Collider Physics, Tokyo, 1994.
- [21] S.D. Drell and T.M. Yan, Phys. Rev. Lett. **24** (1970) 181.
- [22] R. Ragazzon and D. Treleani, Phys. Rev. **D53** (1996) 55.  
 A.H. Müller and H. Navelet. Nucl. Phys. **B282** (1987) 727.
- [23] UA8 Collaboration: R. Bonino *et al.*, Phys. Lett. **B211** (1988) 239.  
 UA8 Collaboration: A. Brandt *et al.*, Phys. Lett. **B297** (1992) 417.
- [24] S.J. Brodsky and J.F. Gunion, Phys. Rev. Lett. **37** (1976) 402.
- [25] N.G. Antoniou, E.N. Argyres, P.S. Dimitriadis, L.B. Papatsimpa and A. Valadakis, Phys. Lett. **B177** (1986) 437.
- [26] J.L. Hewett and T.G. Rizzo, Phys. Rep. **C183** (1989) 193.
- [27] R. Foot and O. Hernández, Phys. Rev. **D41** (1990) 2283.  
 R. Foot, O. Hernández and T.G. Rizzo, Phys. Lett. **B246** (1990) 183; Phys. Lett. **B261** (1991) 153.
- [28] T.G. Rizzo, Phys. Rev. **D48** (1993) 4470.



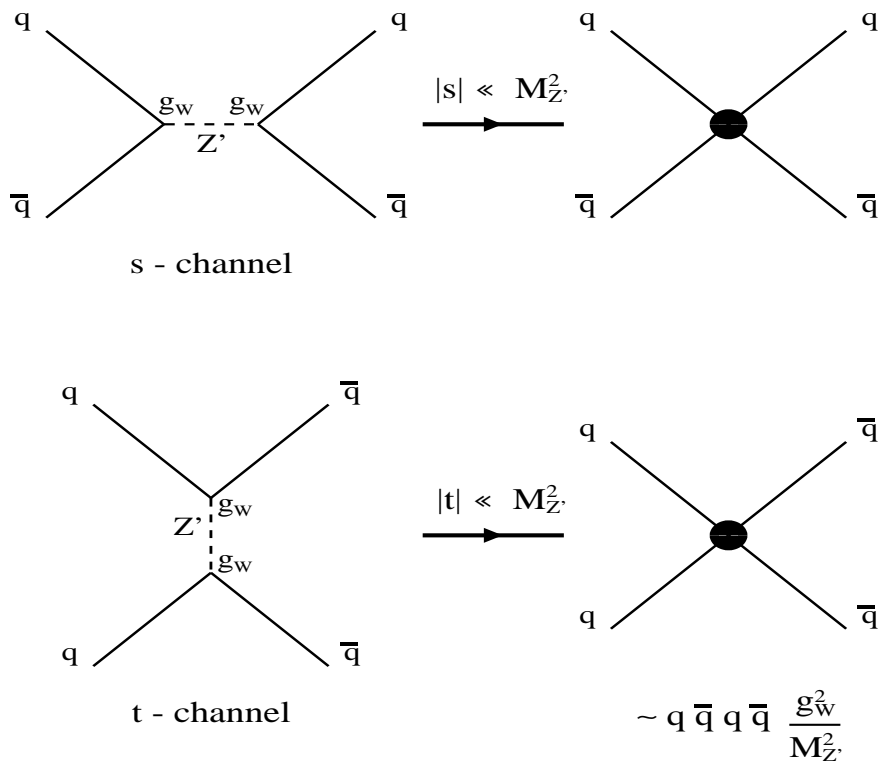


Figure 1: The  $s$ - and  $t$ -channel contributions according to  $Z'$  exchange (left side). For  $|s|$  and  $|t|$  being small, the  $Z'$  acts like an effective contact interaction with relative strength  $\sim \alpha_W/M_{Z'}^2$ , (right side).

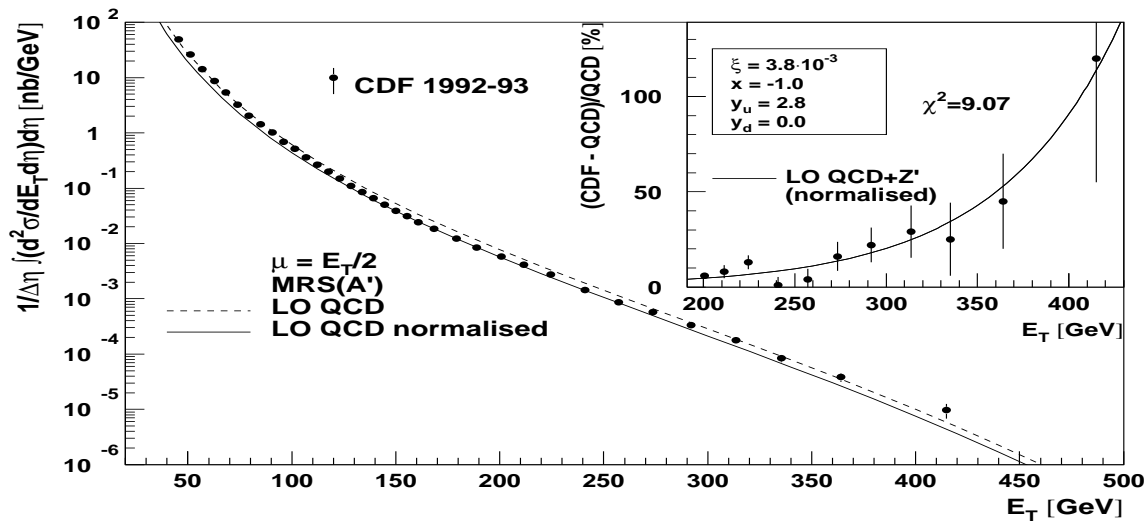


Figure 2: LO calculation of the single inclusive jet cross section (dashed line) and the normalised LO fit (solid line) to the CDF 1992–93 data [1] (as discussed in the text). The small inset shows the difference in per cent between our calculation and the measured cross sections by the CDF Collaboration. Also shown is the *best-fit* of the included  $Z'$  model with the parameters also presented (cf. Section 3.1).

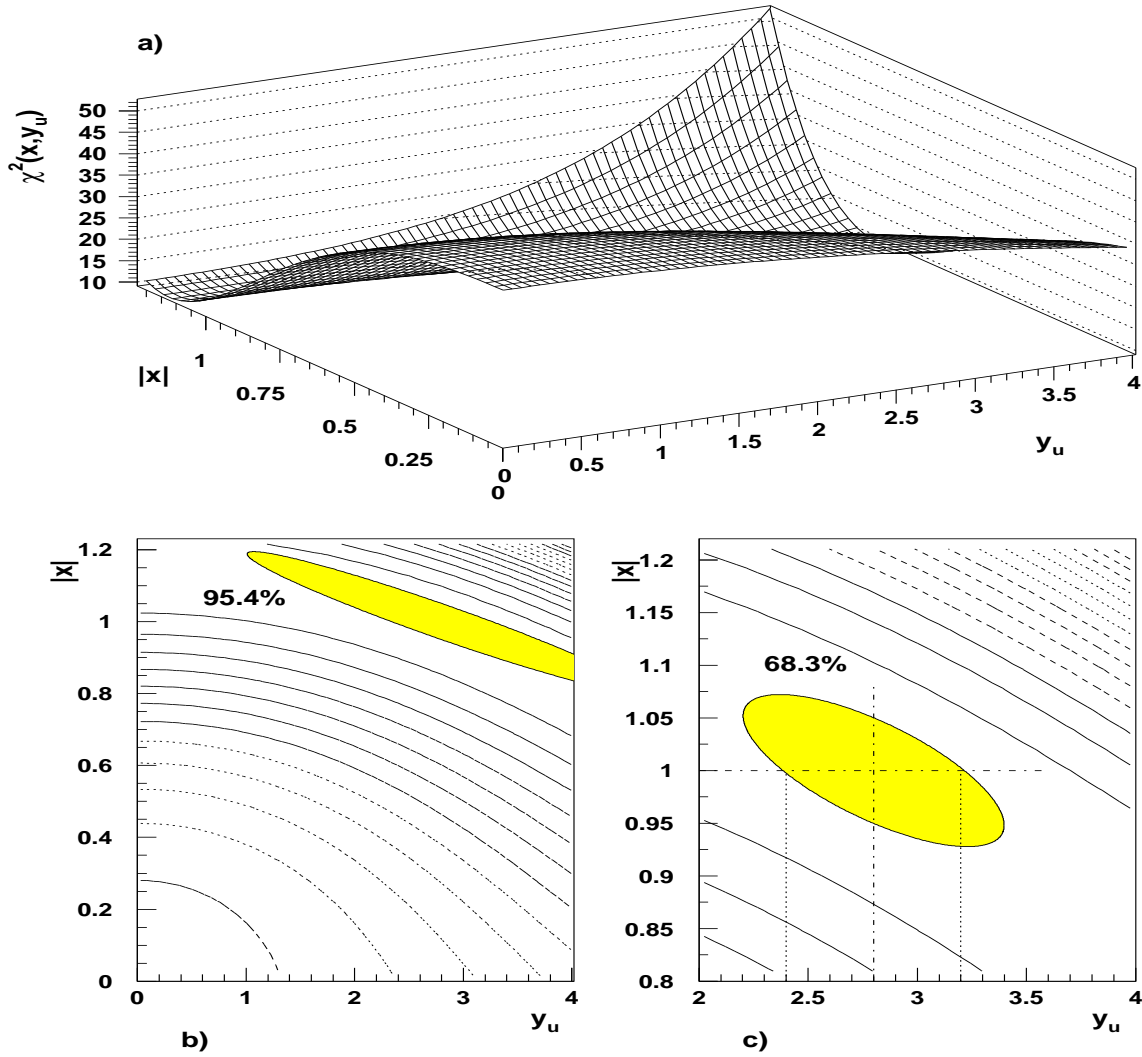


Figure 3: The statistical results of our  $Z'$  analysis: (a) the  $\chi^2$  distribution as a function of the two degrees of freedom  $x$  and  $y_u$  (the fitted parameters), (b) the 95.4% confidence ellipse and (c) the 68.3% confidence ellipse with the central values  $x = -1.0$  and  $y_u = 2.8$  being indicated (best-fit values).

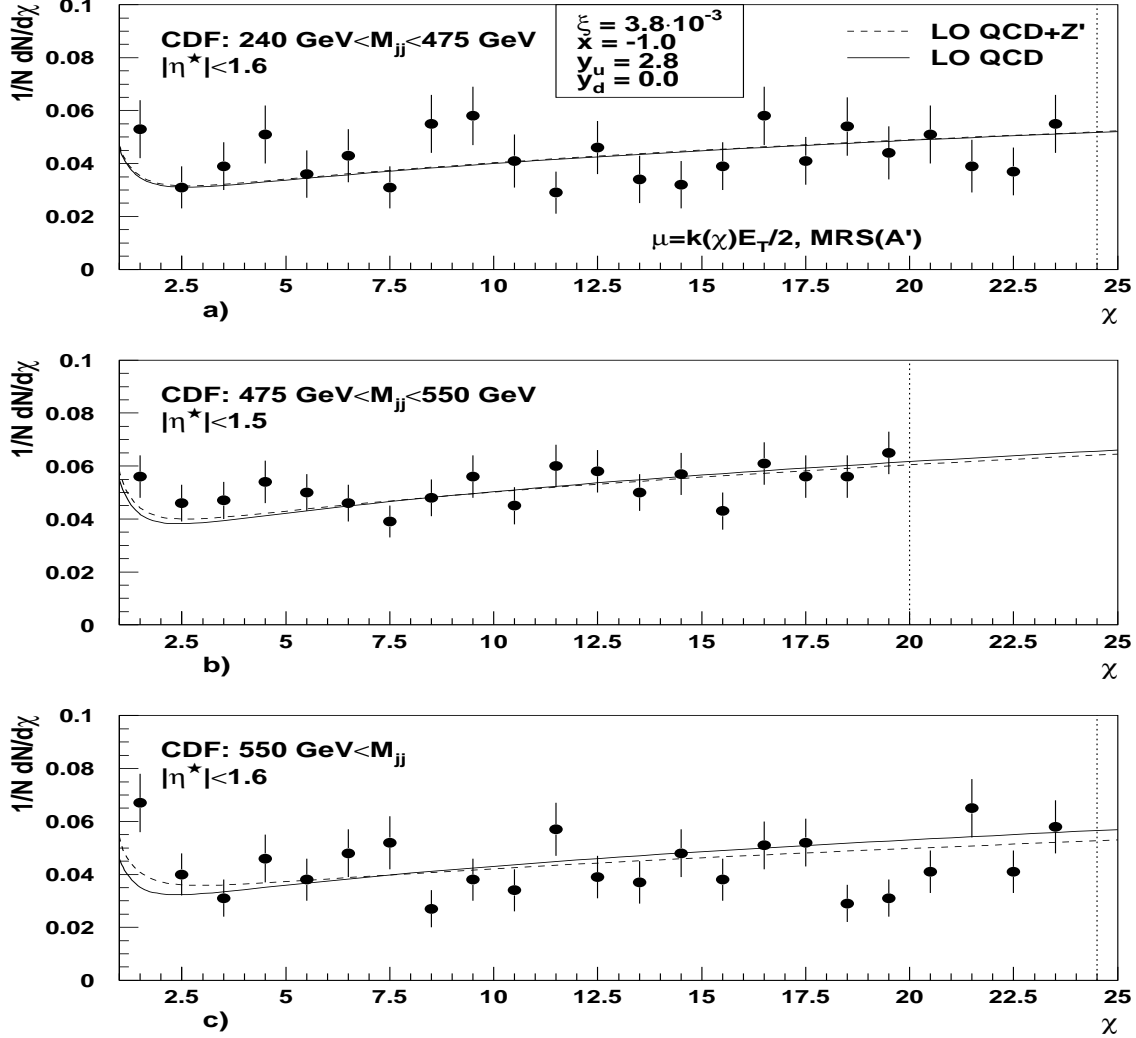


Figure 4: The normalised dijet cross sections at  $\mathcal{O}(\alpha_S^2)$  for pure QCD (solid lines) and the additionally coupled vector boson  $Z'$  (dashed lines) in three different dijet mass bins: (a)  $240 \text{ GeV} < M_{jj} < 475 \text{ GeV}$ , (b)  $475 \text{ GeV} < M_{jj} < 550 \text{ GeV}$  and (c)  $M_{jj} > 550 \text{ GeV}$ . The numerical results are compared to the CDF '92 measurements [17]. The kinematical constraints on  $\eta^*$  and the normalisation intervals in  $\chi$  are indicated and discussed in the text. All  $Z'$  calculations were performed for the central parameter fit:  $x = -1.0$  and  $y_u = 2.8$ . As renormalisation scale we have chosen  $\mu = k(\chi)E_T/2$  from Ref. [16].

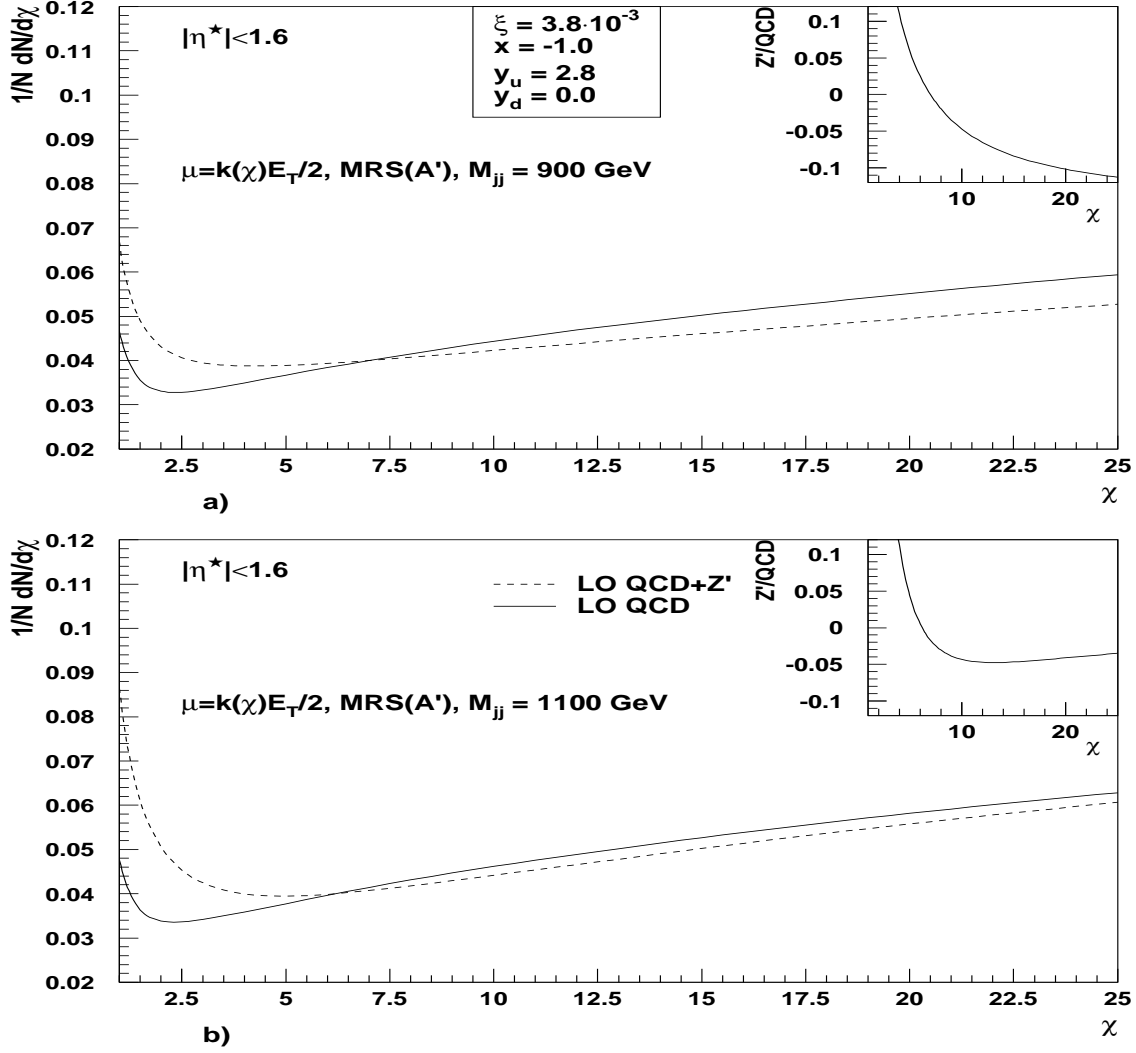


Figure 5: Same as Fig. 4, but now for the two fixed dijet mass bins: (a)  $M_{jj} = 900$  GeV and (b)  $M_{jj} = 1100$  GeV. The dijet cross sections are normalised to unity in the interval  $1 \leq \chi \leq 24.5$ . The relative contributions of the  $Z'$  to the LO QCD calculations ( $Z'/\text{QCD}$ ) are also presented.

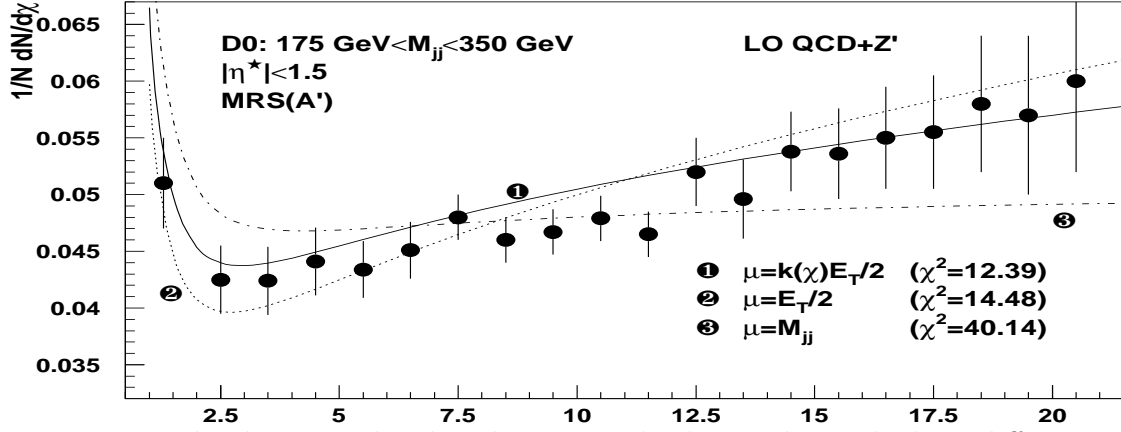


Figure 6: The dijet angular distributions in leading order with three different renormalisation scales including the scale defined in Eq. (9) and employed throughout this section. The cross sections are integrated over  $M_{jj}$  in the range  $175 \text{ GeV} < M_{jj} < 350 \text{ GeV}$ . As before we present the *normalised* cross sections but now for the LO QCD+ $Z'$  calculation only. The results are compared to the data taken from the D0 '94 measurements [20].

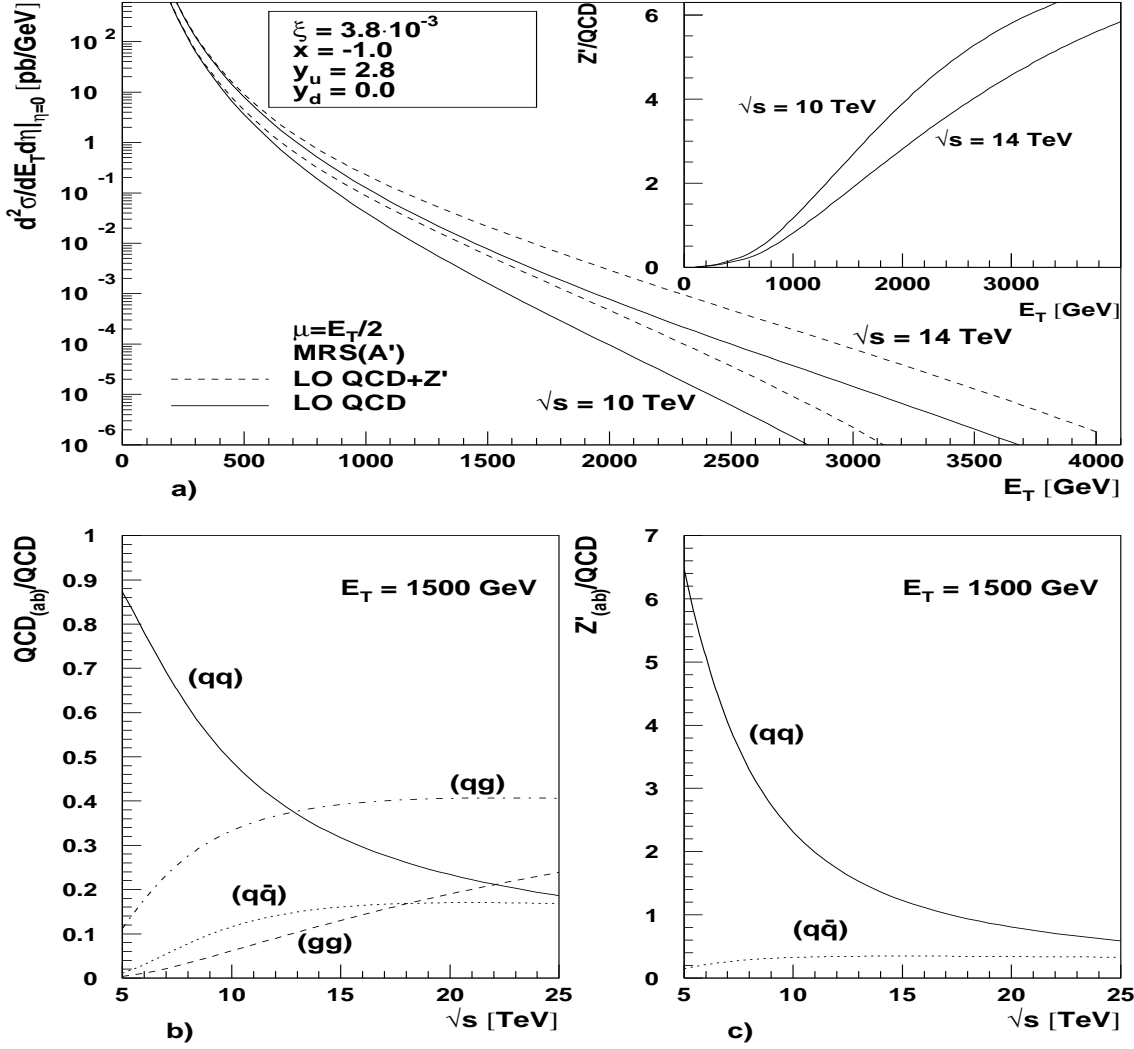
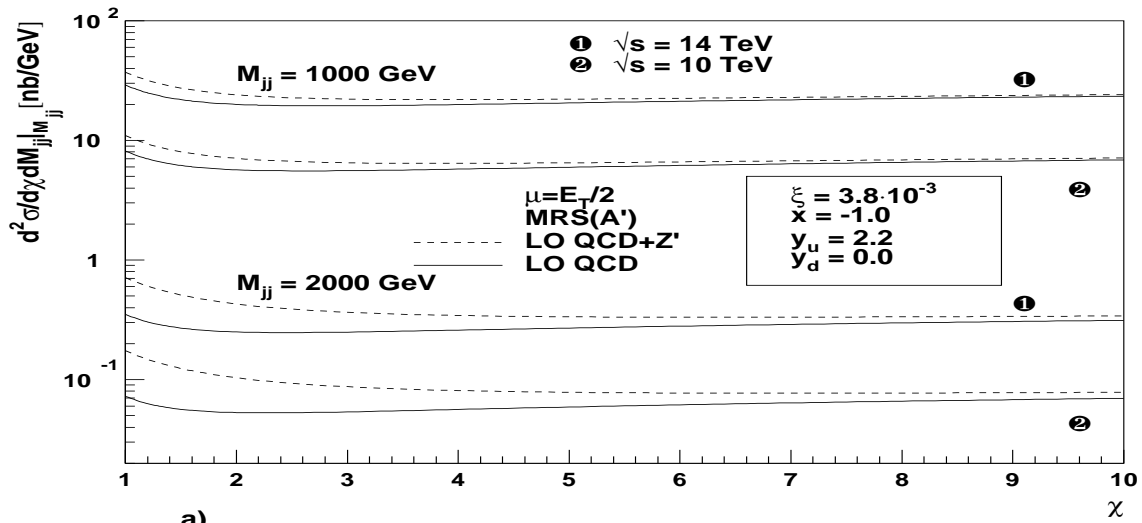
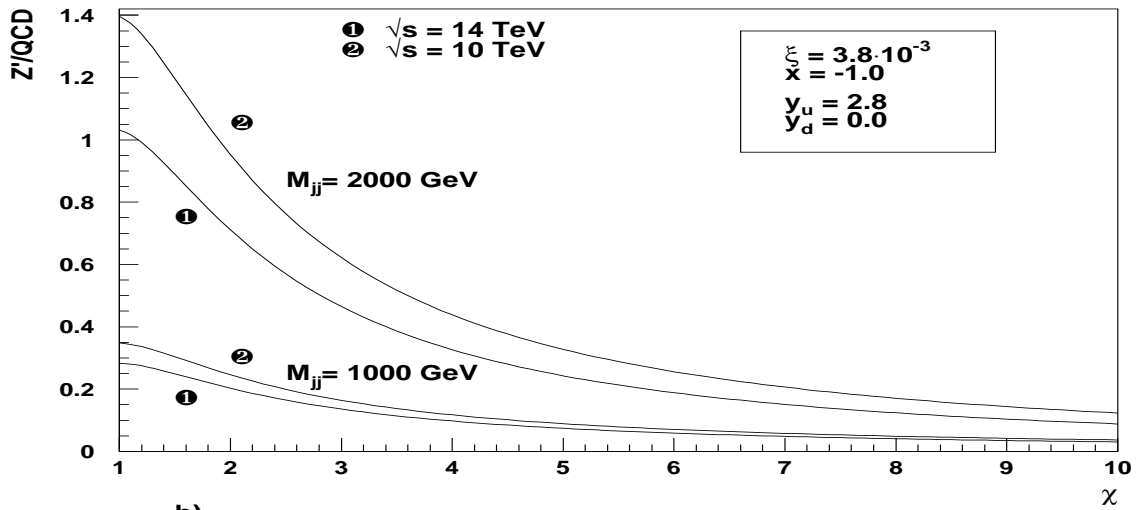


Figure 7: LO calculation of the single inclusive jet cross sections at the LHC for the two centre-of-mass energies 10 TeV and 14 TeV. The ratios  $Z'/\text{QCD}$  are shown in the inset of (a). The contributions of the different subprocesses  $ab \rightarrow cd$  for (b) LO QCD and (c)  $Z'$ , normalised to the full LO QCD calculation, as a function of the centre-of-mass energy are shown. The transverse jet energy was fixed to be  $E_T = 1500$  GeV.



a)



b)

Figure 8: The dijet angular distributions at the LHC for two different invariant dijet masses. The unnormalised cross sections are shown in (a) for LO QCD and LO QCD+ $Z'$ . In (b) we show the corresponding ratios  $Z'/\text{QCD}$  again for the central fit parameters of the  $Z'$  model.



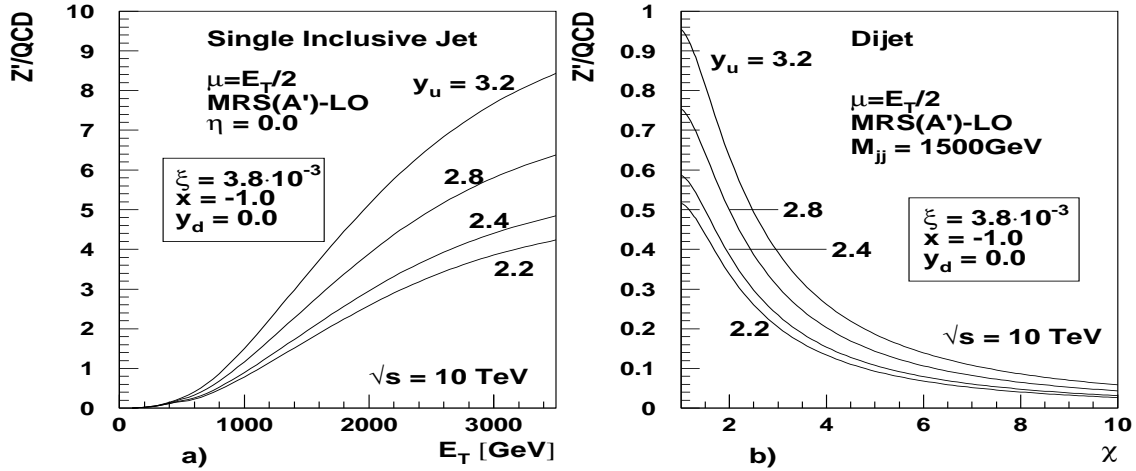


Figure 9: The ratios  $Z'/\text{QCD}$  for the (a) single inclusive jet cross sections ( $\eta = 0$ ) and (b) dijet angular distributions ( $M_{jj} = 1500 \text{ GeV}$ ) at the LHC. We keep  $x, y_d, \xi$  and  $M_{Z'}$  fixed to the values of our best-fit and vary  $y_u$  according to the 68.3% confidence ellipse shown in Fig. 3c. We also present the calculations for the best-fit value  $y_u = 2.2$  of Altarelli *et al.* [7].